Dentomaxillofacial Radiology (2014) 43, 20140080

birpublications.org/dmfr

RESEARCH ARTICLE

Tooth shape reconstruction from dental CT images with the region-growing method

[1]R Yanagisawa, [1]Y Sugaya, [2]S Kasahara and [1]S Omachi

[1]*Graduate School of Engineering, Tohoku University, Sendai, Japan;* [2]*Graduate School of Dentistry, Tohoku University, Sendai, Japan*

Objectives: The three-dimensional shape information of teeth provides useful information. However, obtaining accurate three-dimensional shapes of teeth is difficult without extracting them physically. In this study, we aimed to develop a method for automatically extracting accurate three-dimensional shapes of teeth from dental CT images.
Methods: The proposed method includes pre-processing and region extraction. Pre-processing is a combination of image-processing techniques that enhances tooth regions. In the region-extraction process, the region-growing method is introduced for extracting a region of each tooth. Constraint conditions determined by considering the characteristics of the structure of teeth are introduced for accurate extraction. Finally, morphological image processing is applied for eliminating discontinuous points.
Results: We carried out an experiment in which the three-dimensional shapes of teeth were reconstructed from dental CT images. Quantitative evaluation was performed by measuring the three-dimensional spatial accordance rates between the region obtained by the proposed method and the manually extracted region. The proposed method was significantly more accurate than an existing method at the 5% level.
Conclusions: The experimental results showed that the proposed method reconstructs the shapes of teeth with high precision. However, an unextracted region remained at the surface of the enamel. Solving this problem and improving the extraction accuracy are important topics for future work.
Dentomaxillofacial Radiology (2014) **43**, 20140080. doi: 10.1259/dmfr.20140080

Cite this article as: Yanagisawa R, Sugaya Y, Kasahara S, Omachi S. Tooth shape reconstruction from dental CT images with the region-growing method. *Dentomaxillofac Radiol* 2014; **43**: 20140080.

Keywords: Cone-beam CT; computer-assisted three-dimensional imaging; image reconstruction

Introduction

The three-dimensional shape information of teeth provides useful information for processes such as constructing a tooth database, implant dentistry and disease detection. In this article, we propose a method for automatically extracting the accurate three-dimensional shapes of teeth from dental CT images obtained by a dental micro-CT system.[1]

Numerous image-processing techniques for dealing with tooth images have been proposed. Hereafter, we use the term contour in the sense that it is used in the field of image processing to represent the outline of something in an image. Mol and van der Stelt[2] proposed a method for detecting the change in bone to the morbid state by using the edge extracted from an X-ray image. Jain and Chen[3] proposed a method for identifying individuals by using dental radiographic images, in which a semi-automatic contour extraction method was proposed and the contours of the teeth were used for identification. They improved their method by utilizing both the contour of the teeth and the shapes of dental work such as fillings and bridges;[4] however, this method can only utilize the visible tooth region. Hirogaki et al[5] proposed

Correspondence to: Professor Shinichiro Omachi. E-mail: machi@ecei.tohoku.ac.jp
Received 10 March 2014; revised 28 April 2014; accepted 30 April 2014

a method for reconstructing a three-dimensional dental cast model with a line laser, and Gao et al[6] proposed a method for using shadow speckles for reconstructing three-dimensional shapes. Three shape-from-shading techniques were evaluated by Carter et al[7] for tooth reconstruction, whereas a method for segmenting and visualizing all of the teeth with CT images was proposed by Akhoondali et al.[8] Bors et al[9] proposed an interpolation method aimed at obtaining an n-dimensional object from a set of $(n-1)$-dimensional objects; although they applied their proposed method to the reconstruction of the three-dimensional tooth shape with two-dimensional CT images, the tooth regions were segmented manually. Bro-Nielsen et al[10] developed an interactive tool for segmentation and visualization of the teeth in CT scans by using the region-growing method iteratively to find the non-processed region. Dong-ri and Fu-yuan[11] applied the region-growing method for extracting the region of all the teeth. Buchaillard et al[12] proposed a three-dimensional statistical model for a tooth comprising a mean shape and deformation models with the objective of obtaining a good estimate of the entire tooth when only partial information of a tooth is provided. However, these existing methods are not appropriate for reconstructing the three-dimensional shape of each tooth. Obtaining the accurate three-dimensional shapes of teeth without extracting them physically is difficult using the existing methods.

Omachi et al[13,14] proposed a method for extracting the three-dimensional shapes of teeth from dental CT images semi-automatically with the active contour model. A user determines an initial contour of a tooth in a CT image manually, and the three-dimensional shape of the tooth is reconstructed by propagating the contour to the adjacent images. However, it is difficult to extract the accurate shape of the target tooth using this method because the adjacent teeth or the surrounding tissue is also extracted. This is because the intensity values of the CT images in the target tooth and the alveolar bone around the root of the tooth, or the adjacent teeth around the crowns of the teeth, are quite similar.

In the proposed approach, the region-growing method[15] is introduced for detecting the tooth region. The region-growing method is a technique for expanding regions by aggregating neighbouring pixels or voxels starting from a pixel or voxel called a seed. This technique has been applied in various fields, including medical imaging technologies. Furthermore, Yau et al[16] used region growing for segmenting the inferior alveolar nerve, Kumar et al[17] proposed a method for segmenting the liver and tumour and Palomera-Pérez et al[18] applied this method for blood vessel segmentation.

We previously proposed the idea of using the region-growing method in conference proceedings.[19] The contribution of this article is to present a whole algorithm for reconstructing the three-dimensional shapes of teeth based on this idea and to present the experimental results of this method in comparison with an existing method. The constraint conditions determined by considering the characteristics of the structures of teeth are newly introduced. In addition, region competition is introduced between the target tooth and the adjacent teeth for accurate extraction. Therefore, the proposed method can automatically extract the accurate three-dimensional shapes of teeth.

Methods and materials

Pre-processing

In dental CT images, tooth regions have a tendency to show dispersion of brightness values in many tissues such as the enamel and dental pulp. However, the target region should contain consistent brightness values to distinguish it from other regions. Therefore, conversion of the brightness values facilitates the extraction of the regions from dental CT images. In the proposed method, we introduce normalization of the brightness value based on slice energy (SE),[20] which gives a uniform distribution of brightness to every tissue. We define the x-axis and y-axis as horizontal axes and the z-axis as a vertical axis, as shown in Figure 1. The SE (z) is the summation of brightness values of each slice on the x-y plane. Dispersion of the distribution of the brightness value in a tissue is reduced by normalizing each SE (z), so that all values are the same (standard SE)

Subsequently, contrast enhancement is applied. Generally, when extracting a certain region from an image, accurate extraction can be achieved when a large

Figure 1 Sliced dental CT images in three directions: (a) y-z axial plane, (b) x-z axial plane and (c) x-y axial plane.

difference in brightness values exists between the target and the surrounding regions. However, the obtained image does not always have an appropriate property for extraction because the surrounding tissues, such as the alveolar bone, gum and periodontal ligament, tend to show a distribution of brightness values that is similar to the tooth region to some extent. On the other hand, the tooth region has relatively high brightness values compared with the surrounding tissues. Based on this consideration, to enhance the brightness value of the region that has a high probability of being the tooth region, the brightness value of each voxel was replaced by a square.

The next step is smoothing. When a CT image is obtained, noises that are specific to CT images generally occur. The bilateral filter,[21] which is one of the edge-preserving smoothing filters, is introduced in the proposed method. This filter achieves strong smoothing between two voxels if the following condition is met: the distance from one voxel to the other is short or these voxels have similar brightness values. By introducing this smoothing method, noise reduction and preservation of the edge information are achieved simultaneously.

Region extraction

On the CT image, the dental pulp has a quite low brightness value, the dentine has a relatively high brightness value and the enamel has the highest brightness value in a tooth. The proposed method extracts the region of a tooth from CT images with the region-growing method considering these characteristics of the CT image. A simple overview of the region-growing method is shown in Figure 2. In this figure, each small square is a voxel, and the area surrounded by the thick lines represents the growing region. First, a seed is determined inside a tooth, and the initial region is defined to include only one voxel of the seed, as shown in Figure 2a. Subsequently, the voxels with certain characteristics are gradually aggregated as one connected region, as shown in Figure 2b–f. As a general rule, brighter voxels are gradually aggregated starting from a dark voxel. Some constraint conditions are incorporated for accurate extraction. Note that although Figure 2 is shown in two dimensions for simplicity, the proposed method searches for voxels in the three-dimensional space.

A seed must be detected in a tooth at the beginning of the region-growing method, and this should be a characteristic point of the target region to achieve accurate extraction. Since the dental pulp is on the central axis of a tooth and is a particular tissue, the proposed method sets the seed on the dental pulp automatically. We selected the voxel for which the brightness value is the minimum as the seed because the dental pulp has a low brightness value. First, the user indicates one voxel in a target tooth, and this voxel is regarded as the initial tentative seed. Voxels with a lower brightness value are searched iteratively from the neighbouring region of the tentative seed to determine the voxel for which the brightness value is the minimum.

After detecting the seed, the region-growing method is applied by using this seed as the starting point. The dental pulp, dentine and enamel of each tooth are the tissues that are expected to be extracted, and a major characteristic of these tissues is that the brightness value of a voxel increases as it approaches the surface of

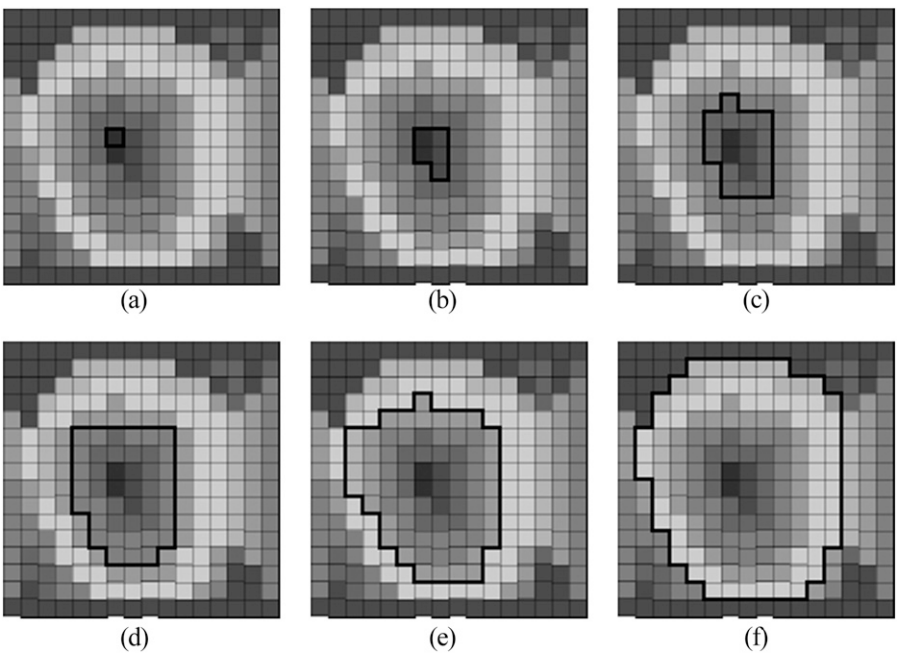

Figure 2 The region-growing method. Each small square is a voxel, and the region surrounded by the thick lines represents a growing region. (a) Initial region. (b–f) Growing region.

a tooth. Considering this characteristic, the proposed method is able to extract the target tissues as one connected region by gradually aggregating voxels with higher brightness values from the dental pulp. However, overextraction may occur or the process may fall into the local minimum if we simply aggregate voxels with higher brightness values. To solve this problem, the proposed method introduces three constraints for aggregating voxels. Voxel aggregation is performed when all of these three conditions are satisfied.

(1) Constraint by the continuity of brightness values: as described above, the proposed method extracts a tooth region by setting the seed on the dental pulp and gradually aggregating neighbouring voxels with higher brightness values. However, the differences in the brightness values at the boundary between the dental pulp, dentine and enamel are relatively large. Therefore, when the brightness value of the candidate voxel for aggregation is higher than the current voxel, the allowable difference, d_h, between the brightness values of these voxels should be large. On the other hand, the enamel, which consists of the tooth surface, has a very high brightness value compared with its outside tissues. To suppress overextraction of the outside tissues, when the brightness value of the candidate voxel for aggregation is lower than the current voxel, the allowable difference, d_l, between the brightness values of these voxels should be small. We define d_h and d_l as follows:

$$d_h = \left(255 - \frac{I_{current} + I_{previous}}{2}\right) \times \alpha + \beta$$

$$d_l = (I_{previous} - I_{current}) \times d_h \times \gamma + \delta$$

where $I_{current}$ and $I_{previous}$ are the brightness values of the current voxel and its parental voxel, respectively, and α, β, γ and δ are parameters. In case that $d_h < 0$ or $d_l < 0$, these values are determined to be zero. With these values, the upper limit L_{t1} and lower limit L_{b1} of growth are calculated by the following equations:

$$L_{t1} = I_{current} + d_h$$

$$L_{b1} = I_{current} - d_l$$

(2) Constraint by the maximum brightness value: some voxels in the enamel do not have very high brightness values, and the change in the brightness values from these voxels to the gum is relatively small and is somewhat continuous. Hence, a risk of overextracting the gum exists. To avoid this overextraction, we introduced a constraint condition defined by the degree of progress of the region-growing process, where the maximum brightness value in the extracted region is used as the degree of progress. This constraint determines the lower limit of the brightness value of the voxels that can be aggregated as follows:

$$L_{b2} = \begin{cases} \dfrac{I_{Th1} - I_{Th2}}{255} I_{max} + I_{Th2} & \left(\text{if } I_{max} > -\dfrac{255 \times I_{Th2}}{I_{Th1} - I_{Th2}}\right) \\ 0 & (\text{otherwise}) \end{cases}$$

where I_{max} is the maximum brightness value in the region that has already been extracted and I_{Th1} and I_{Th2} are parameters, and L_{b2} is the lower limit of the brightness value. Overextraction must be suppressed when the growth reaches the dentine, and the value of the lower limit becomes large according to the degree of growth progress. On the other hand, I_{Th1} should be determined not to affect the lower limit on extracting the enamel.

(3) Constraint by isobrightness contour information: to suppress overextraction where the target tooth touches other teeth or the surrounding tissues, a constraint considering the isobrightness of the contours is imposed. These contours are obtained from an x-y axial sliced image by tracing voxels with the same brightness value. We define the contour strength at a voxel as the number of contours that are drawn at this voxel by changing the threshold from 1 to 255. We define the lower limit, L_{b3}, for the growing region of this constraint as follows:

$$L_{b3} = \frac{I_{Th3} - I_{Th4}}{255} \times I_{contour} + I_{Th4}$$

where $I_{contour}$ is the value of the contour strength and I_{Th3} and I_{Th4} are parameters. As the probability of the existence of the isobrightness contour increases, the stringency of the constraint that is to be applied on region growing should also increase. By introducing this constraint, the shape information of the surface of the target tooth region is retained.

These three constraint conditions can achieve suppression of overextraction of the alveolar bone around the root of a tooth. However, concern remains that the adjacent teeth around the crown of the tooth will be overextracted. This can be attributed to the fact that the alveolar bone has a slightly lower brightness value compared with the tooth region around the crown, and, on the other hand, the adjacent teeth have a similar or higher brightness value than that of the target tooth. To solve this problem, the proposed method introduces a competition process by regions grown from plural seeds and defines an obvious boundary between the target tooth and the adjacent teeth. An example is shown in Figure 3. Suppose that the tooth regions given in Figure 3a include the target tooth; in this situation, the target tooth region is in contact with the adjacent regions. The result obtained when the regions are

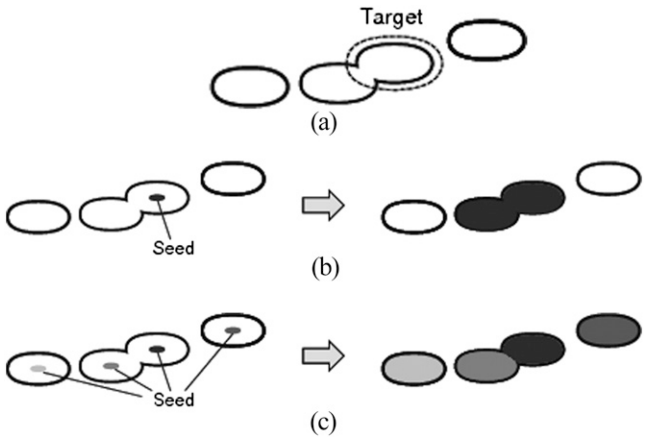

Figure 3 Labelling. (a) Input image. (b) Labelling with a single seed. (c) Labelling with plural seeds.

labelled with a single seed is shown in Figure 3b. When only one seed is given, overextraction of the adjacent regions may occur because the edge of the target region at the contacted position is exceeded. The result obtained when plural seeds are set on the target tooth region and surrounding regions is shown in Figure 3c. When plural seeds are applied, an appropriate boundary is defined by competition of the plural regions.

For region competition, two kinds of belonging degrees are defined. One is defined by the adjacency to each region that has already been extracted, and this is given as follows:

$$n_i = \sum_{j \in R_i} \frac{1}{d_j}$$

where i is a label assigned to an extracted region, R_i is a set of voxels belonging to the region and d_j is the distance between voxel j and the target voxel. If many near voxels exist, the value n_i will become large. The other is defined by the distance to the centroid of each region, and this is given as follows:

$$l_i = \left| \frac{1}{\boldsymbol{x}_{\mathrm{centroid}_i} - \boldsymbol{x}_{\mathrm{object}}} \right|$$

where $\boldsymbol{x}_{\mathrm{object}}$ is the position of the target voxel and $\boldsymbol{x}_{\mathrm{centroid}_i}$ is the centroid of region i. This value becomes large when the target voxel is far from the centroid of a certain region. The total belonging degree to each region of the target voxel is calculated by

$$b_i = r \times n_i + s \times l_i$$

where r and s are the weights of these belonging degrees. The region with the largest belonging degree will aggregate at this target voxel.

In general, the region extracted by the region-growing method has discontinuous points owing to remaining noise on the image. Therefore, morphological image processing is introduced after applying region growing and region competition to remove these discontinuous points. We repeated the closing process with a 3×3 structure element for $n_{\mathrm{iteration}}$ times.

Results

To illustrate the effectiveness of the proposed method, we carried out experiments in which the three-dimensional regions of the target teeth were extracted from dental CT images. The left-side lower central incisors, right-side lower central incisors, left-side lower lateral incisors, right-side lower lateral incisors, left-side lower canine teeth and right-side lower canine teeth were used as the target teeth. The parameters used in the experiments are shown in Table 1.

To our knowledge, no method exists that automatically reconstructs a three-dimensional tooth shape. Therefore, the semi-automatic method[13,14] was adopted as the existing method, and the results were compared quantitatively. Note that the user should manually provide a rough tooth shape in a slice of the CT images for the existing method, whereas the user should indicate only one voxel in a tooth for the proposed method.

Quantitative evaluation was performed by measuring the three-dimensional spatial accordance rates between the region obtained by the proposed method and the

Table 1 Parameter values used for the experiments

Process	*Parameter name*	*Value*
Pre-processing	Standard slice energy	180,000
Region growing	α	1.0
	β	5.0
	γ	0.1
	δ	5.0
	I_{Th1}	255.0
	I_{Th2}	−100.0
	I_{Th3}	0.0
	I_{Th4}	30.0
	r	1.0
	s	1.0
	$n_{\mathrm{iteration}}$	7.0

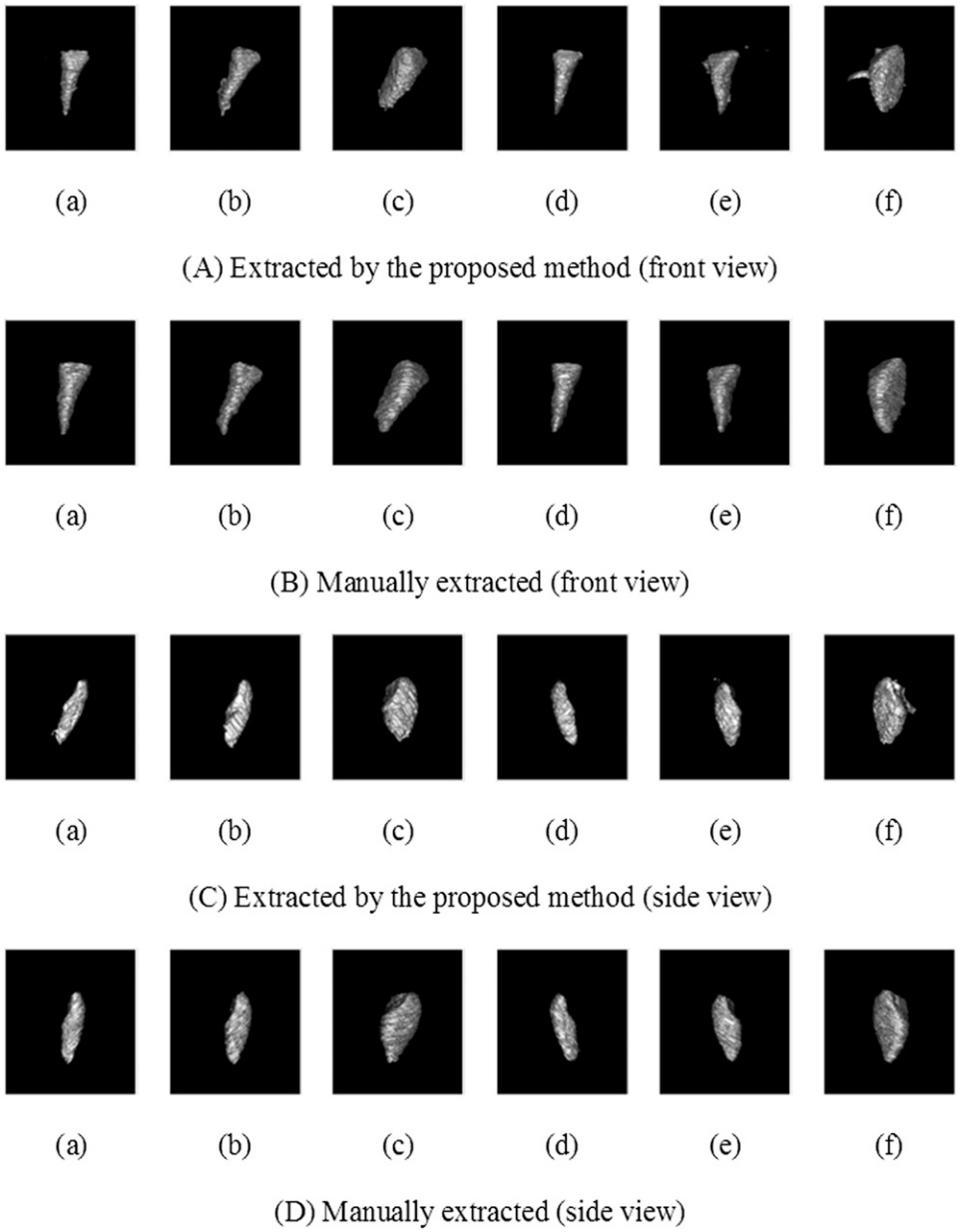

Figure 4 (A, C) Results obtained by the proposed method. (B, D) Manually extracted shapes. (a) 31, (b) 32, (c) 33, (d) 41, (e) 42 and (f) 43. The two digit numbers are the FDI notations.

manually extracted region. For this purpose, the precision, recall and *F*-measure values were defined as follows:

$$\text{Precision} = \frac{\text{Match}}{\text{Result}}$$

$$\text{Recall} = \frac{\text{Match}}{\text{True}}$$

$$F\text{-measure} = \frac{2 \times \text{Precision} \times \text{Recall}}{\text{Precision} + \text{Recall}}$$

True represents the correct region that should have been extracted, and this region was determined manually. Result represents the region extracted by the proposed method and Match represents the overlapping region of these regions. The precision value is an indicator for measuring the degree of suppression of overextraction. On the other hand, the target region is covered finely if the recall value is large.

The three-dimensional shapes of the teeth that were reconstructed by the proposed method, along with the manually extracted shapes, are shown in Figure 4. This figure shows that the proposed method could reconstruct the three-dimensional shapes of the teeth. The

Table 2 Precision, recall and *F*-measure of the proposed method and the existing method

	Proposed method			*Existing method*		
Tooth (FDI notation)	*Precision*	*Recall*	F-*measure*	*Precision*	*Recall*	F-*measure*
31	0.966	0.830	0.893	0.602	0.635	0.618
32	0.911	0.857	0.883	0.485	0.888	0.627
33	0.978	0.850	0.910	0.808	0.966	0.880
41	0.939	0.847	0.891	0.294	0.958	0.450
42	0.923	0.828	0.873	0.673	0.909	0.773
43	0.939	0.847	0.891	0.804	0.965	0.877
Average	0.943	0.843	0.890	0.611	0.887	0.704

precision, recall and *F*-measure values are summarized in Table 2. This table shows that the precision of the proposed method was very high, and the *F*-measures of the proposed method were higher than those of the existing method for all of the teeth. The statistical significance of the *F*-measure values was tested by using a paired *t*-test, and the resulting *p*-value of 0.041 indicated that the proposed method was significantly more accurate compared with the existing method at the 5% level.

The three-dimensional shapes of the lower central incisors were extracted finely, as shown in Figure 4a,d. The precision values of these teeth were very high, confirming that overextraction was suppressed by the proposed method. A small degree of overextraction occurred for the lower lateral incisors, especially for the right side around the root (Figure 4b,e). Although the shapes were reconstructed finely for the canine teeth, a small degree of overextraction of the right-side lower first pre-molar at the crown of the right-side lower canine tooth was observed (Figure 4c,f). This occurred because the pre-molars were not the target teeth in this experiment, and this problem could be solved easily by introducing more new seeds on the pre-molars.

From these evaluations and considerations, we conclude that the proposed method can achieve extraction with suppression of overextraction, which is a major issue for the existing method, at the roots and crowns of the teeth. We believe that two major factors should be considered to explain the ability of the proposed method to achieve extraction with suppression of overextraction. First, overextraction of the alveolar bone was finely suppressed by introducing three active constraints for region growing. Second, a defining boundary was generated by the introduction of region competition at the contact points between the target tooth and the adjacent teeth. On the other hand, the recall value was relatively low, which means that the region should be extracted.

Finally, we compared the extracted shapes of the proposed method and the existing method. The three-dimensional shapes of the left-side lower central incisor reconstructed by the proposed method and the existing methods are shown in Figure 5. A large degree of overextraction of the surrounding region was apparent when the existing method was applied. Overextraction occurred at the crown of the tooth, where the tooth was in contact with the adjacent teeth. Therefore, it can be concluded that the existing method is sensitive to the characteristics of the surrounding tissues, whereas the proposed method adequately suppresses the influence of the surrounding tissues.

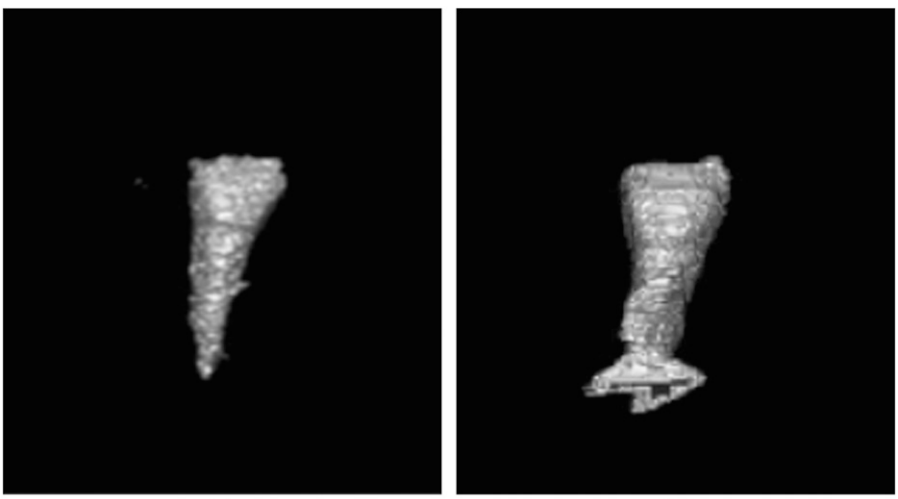

Figure 5 Reconstructed three-dimensional shapes of a tooth. (a) Proposed method. (b) Existing method.

Conclusions

In this article, a method for reconstructing the three-dimensional shape of a tooth from dental CT images obtained by a micro-CT system was proposed. In the proposed method, the region-growing method for extracting the region of a target tooth was introduced. Normalization, contrast enhancement and smoothing were introduced as pre-processing steps for achieving accurate extraction. Normalization was used to reduce the variance of the brightness values along the *z*-axis, and contrast enhancement was introduced to emphasize the boundary between the tooth region and the surrounding tissues. The bilateral filter was introduced as a smoothing filter to reduce the particular noise of CT images. Next, the region-growing method was applied with three constraints defined by the continuity of the brightness values, the maximum brightness value and isobrightness contour information. These constraints suppressed overextraction, which is a major issue when using the existing method. Subsequently, region competition was performed by growing regions from plural seeds, which determined an obvious boundary between the target tooth and the adjacent teeth. Finally, morphological image processing was applied for eliminating discontinuous points after the region-growing method was applied.

The experimental results showed that three-dimensional teeth shapes could be reconstructed by using the proposed method with high precision values. However, a thin layer of unextracted region remained at the surface of the enamel on the region extracted by using the proposed method. Solving this problem and improving the extraction accuracy will be important topics in future work.

References

1. Arai Y, Tammisalo E, Iwai K, Hashimoto K, Shinoda K. Development of a compact computed tomographic apparatus for dental use. *Dentomaxillofac Radiol* 1999; **28**: 245–8. doi: 10.1038/sj/dmfr/4600448
2. Mol A, van der Stelt PF. Application of digital image analysis in dental radiography for the description of periapical bone lesions: a preliminary study. *IEEE Trans Biomed Eng* 1991; **38**: 357–9. doi: 10.1109/10.133231
3. Jain AK, Chen H. Matching of dental X-ray images for human identification. *Pattern Recognition* 2004; **37**: 1519–32.
4. Chen H, Jain AK. Dental biometrics: alignment and matching of dental radiographs. *IEEE Trans Pattern Anal Mach Intell* 2005; **27**: 1319–26. doi: 10.1109/TPAMI.2005.157
5. Hirogaki Y, Sohmura T, Satoh H, Takahashi J, Takada K. Complete 3-D reconstruction of dental cast shape using perceptual grouping. *IEEE Trans Med Imaging* 2001; **20**: 1093–101. doi: 10.1109/42.959306
6. Gao J, Xu W, Geng J. 3D shape reconstruction of teeth by shadow speckle correlation method. *Optic Laser Eng* 2006; **44**: 455–65.
7. Carter CN, Pusateri RJ, Chen D, Ahmed AH, Farag AA. Shape from shading for hybrid surfaces as applied to tooth reconstruction. In: *Proceedings of the 17th IEEE International Conference on Image Processing*, 2010. pp. 4049–52.
8. Akhoondali H, Zoroofi RA, Shirani G. Rapid automatic segmentation and visualization of teeth in CT-scan data. *J Appl Sci* 2009; **9**: 2031–44.
9. Bors AG, Kechagias L, Pitas I. Binary morphological shape-based interpolation applied to 3-D tooth reconstruction. *IEEE Trans Med Imaging* 2002; **21**: 100–8.
10. Bro-Nielsen M, Larsen P, Kreiborg S. Virtual teeth: a 3D method for editing and visualizing small structures in CT scans. In: *Proceedings of the Computer and Communication Systems*, 1996. pp. 921–4.
11. Dong-ri S, Fu-yuan G. The segmentation algorithm of dental CT images based on fuzzy maximum entropy and region growing. In: *Proceedings of the International Conference on Bioinformatics and Biomedical Technology*, 2010. pp. 74–8.
12. Buchaillard SI, Ong SH, Payan Y, Foong K. 3D statistical models for tooth surface reconstruction. *Comput Biol Med* 2007; **37**: 1461–71. doi: 10.1016/j.compbiomed.2007.01.003
13. Omachi S, Saito K, Aso H, Kasahara S, Yamada S, Kimura K. Tooth shape reconstruction from CT images using spline curves. In: *Proceedings of the International Conference on Wavelet Analysis and Pattern Recognition*, 2007; pp. 393–6.
14. Omachi S, Saito K, Aso H, Kasahara S, Yamada S, Kimura K. Semi-automatic reconstruction of tooth shape from CT images by contour propagation. [In Japanese.] *IEICE Trans Info Syst* 2008; **J91-D**: 2426–9.
15. Pratt WK. *Digital image processing*. 4th edn. Los Altos, CA: Wiley-Interscience; 2007.
16. Yau HT, Lin YK, Tsou LS, Lee CY. An adaptive region growing method to segment inferior alveolar nerve canal from 3D medical images for dental implant surgery. *Comput Aided Des Appl* 2008; **5**: 743–52.
17. Kumar SS, Moni RS, Rajeesh J. Automatic segmentation of liver and tumor for CAD of liver. *J Adv Info Technol* 2011; **2**: 63–70.
18. Palomera-Pérez MA, Martinez-Perez ME, Benitez-Pérez H, Ortega-Arjona JL. Parallel multiscale feature extraction and region growing: application in retinal blood vessel detection. *IEEE Trans Inf Technol Biomed* 2010; **14**: 500–6.
19. Yanagisawa R, Omachi S. Extraction of 3D shape of a tooth from dental CT images with region growing method. In: *Proceedings of the Fourth International Conference on Computational Forensics*, 2011. pp. 68–77.
20. Grenier T, Revol-Muller C, Costes N, Janier M, Gimenez G. Automated seeds location for whole body NaF PET Segmentation. *IEEE Trans Nucl Sci* 2005; **52**: 1401–5.
21. Tomasi C, Manduchi R. Bilateral filtering for gray and color images. In: *Proceedings of the Sixth International Conference on Computer Vision*, 1998. pp. 839–46.